COBEM 2023 27TH INTERNATIONAL CONGRESS OF MECHANICAL ENGENEERING

ABCM Brazilian Society of Mechanical Sciences and Engineering
27th ABCM International Congress of Mechanical Engineering
December 04-08, 2023, Florianópolis-SC, Brazil

COB-2023-2400
CONTRIBUTIONS TO THE NUMERICAL SIMULATION OF FLOWS IN 180 ° CURVES AND PORTABLE WIND TUNNELS

Matheus de Araujo Siqueira
Bruno Furieri
Jane Meri Santos
Universidade Federal do Espírito Santo, Departamento de Engenharia Ambiental
matheusdearaujo211@gmail.com bruno.furieri@ufes.br jmerisantos@yahoo.com.br

Philipe Uhlig Siqueira
Pontifícia Universidade Católica do Rio de Janeiro
philipe.uhlig@gmail.com

Abstract. *A cause of discussion in the recent literature is about the internal airflow of the portable wind tunnel (PWT). One of the devices used to estimate the emission rate of odorant compounds emitted by passive liquid surfaces. In this scenario, the numerical simulation of the PWT internal airflow is a key tool for its better understanding. Nonetheless, the geometry of the apparatus makes its numerical solution challenging. One of the main questions when simulating the PWT internal airflow is about the reliability of the calculations in the 180° curve. Despite that, there is a lack of experimental data concerning the airflow in this region to validate the numerical solutions. Thus, it was simulated/validated the flow inside a U-Bend which the literature presents reliable experimental velocity measurements. It was tested the use of two different turbulence models, the* $standard\ \kappa - \epsilon$ *and the* $SST\ \kappa - \omega$*. So as the use of the two different mesh types, a structured and a non-structured. These data were used as input to the PWT internal airflow simulations. Notwithstanding the foregoing, when conducting the PWT simulations it was noted that the discretization order of the convective terms of the equations of momentum, turbulent kinetic energy (TKE), and its specific dissipation has a relevant impact on the results. Thus, it was tested the use of a discretization blending factor between the two methods. More accurate results for the U-bend internal flow simulations were obtained when using the* $SST\ \kappa - \omega$ *turbulence model and a structured mesh. To the PWT internal airflow simulations, the results showed that the use of the discretization factor between the first and second-order upwind methods equal to 0.75 has conducted the simulations to convergence maintaining a relatively great accuracy.*

Keywords: *portable wind tunnel , u-bend, computational fluid dynamics, turbulence model, discretization order.*

1. INTRODUCTION

Gaseous compounds emitted to the atmosphere by wastewater treatment plants (WWTP) or landfills can cause health effects, like eye, nose, and throat irritation, headache, nausea, diarrhea, hoarseness, sore throat, cough, among others (Godoi *et al.*, 2018; Hu *et al.*, 2017; Beghi *et al.*, 2012; Yang *et al.*, 2012; Schiffman and Williams, 2005); greenhouse gases effects (Glaz *et al.*, 2016; Daelman *et al.*, 2012) and also annoyance to the nearby population leading to some complaints due to malodorous (Hayes *et al.*, 2014; Gostelow *et al.*, 2001). One of the most relevant sources of odorant compounds in WWTP is passive liquid surfaces. They can be defined as liquid surfaces classified as area sources swept by the atmospheric airflow (Capelli *et al.*, 2009; Lebrero *et al.*, 2011). Examples of passive surfaces in WWTP include primary and secondary settlement tanks and stabilization ponds. To estimate odor emission rates in passive liquid surfaces, different methodologies are being proposed, such as the semi-empiric emission models, inverse dispersion modeling, and the use of equipment that confines a small portion of the emitting surface and takes samples of the air containing the pollutant directly in the emitting surface (Prata Jr *et al.*, 2018). Due to its relatively low cost and easy handling, equipment that enclosure part of the emitting surface is being widely used to estimate odor emission rates. The portable wind tunnel (PWT) is one of those equipment. This device was designed to promote in its main section a repeatable, steady, and parallel airflow, and at its exit a well mixture between the emission and the clean air (Jiang *et al.*, 1995; Jiang and Kaye, 1996). However, its aerodynamic performance is still a cause of discussion (Martins *et al.*, 2018). One of the key tools to better understand the operation of PWTs is the numerical simulation of its inside airflow.

One of the major issues when simulating the airflow inside the PWT proposed by Jiang *et al.* (1995) is to ensure that the calculations along its 180 ° curve are being well performed. Once it evolves an abrupt change of the airflow direction, a higher velocity and pressure gradients, greater formation of vortices, and a sudden modification of a flow majorly $1D$ to a majorly $3D$. Thus, the turbulence model calculations should be able to capture all these features. However, there

aren't experimental measurements of the airflow velocity inside the PWT 180° curve to evaluate the accuracy of the turbulence model calculations. In this way, it was performed the simulation of the flow inside a U-Bend which possesses reliable velocity experimental data presented in the literature (Benson *et al.*, 2020). In this case, it was tested two different methodologies to build the computational mesh, structured and non-structured. Also was tested two different turbulence models, the $standard\ \kappa-\varepsilon$ and the $SST\ \kappa-\omega$. These results were used as input to simulate the airflow inside the PWT, i.e. the best mesh construction methodology and the turbulence model that better adapts to solve the problem. Despite that, when simulating the PWT airflow, issues concerning the convective terms discretization order were encountered. The first-order upwind method produced a great simulation convergence, however with poor accuracy. On the contrary, the second-order upwind method led to convergence issues, but with great accuracy when compared to the experimental data. In an attempt to better deal with this scenario, a discretization blending factor between the two models was tested.

In this way, the present work has the objective to test two different turbulence models to simulate the Benson *et al.* (2020) U-bend flow, the $standard\ \kappa-\varepsilon$ and the $SST\ \kappa-\omega$. To perform the airflow simulation inside the PWT proposed by Jiang *et al.* (1995), it was tested three different discretization methodologies for the equations of momentum, turbulent kinetic energy, and its specific dissipation rate. The first and second order upwind and the use of a discretization blending factor of the first and second order upwind methods.

2. METHODOLOGY

2.1 Domains of interest

The flow inside a U-bend is simulated as a complementary validation using the Benson *et al.* (2020) experimental data. The purpose behind the U-bend simulations is to show that a critical part of the PWT configuration, i.e., its curve, is being well simulated. The U-bend configuration used by the author is shown in Figure 1. Although the fluid used in the Benson *et al.* (2020) experiments was water and the fluid used in the PWT experiments is air, the Reynolds number ($Re = {}^{UL}/_{\nu}$) of both cases is similar and equal to $1.5x10^4$ and $1.9x40^4$, respectively. The experimental data were obtained using magnetic resonance velocimetry.

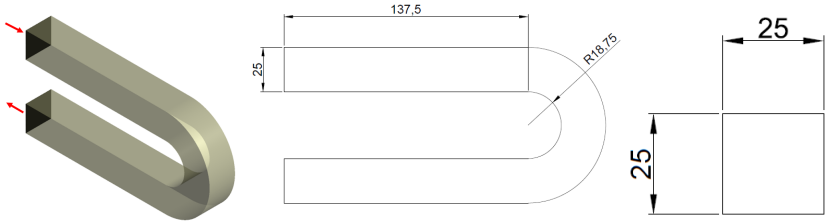

(a) (b) (c)

Figure 1: U-Bend geometry used in the present work: (a) Isometric view; (b) Longitudinal dimensions $[mm]$ and (c) Transversal dimensions $[mm]$.

The reference case is the PWT built based on the design presented by Jiang *et al.* (1995) and shown in Figure 2. The flow of clean air enters the inlet duct and then to the expansion section. The idea of these two parts is to establish a stable and reproducible flow in the main section. The main section of the device is open-bottomed to the emitting surface, i.e. the gas-liquid interface. Hence it is in this region where the emitted odorant compound will be carried by the clean airflow. After the main section, the flow now containing the odorous compound goes to the contraction section which has the objective to improve the mixture between the clean air and the odorous compounds. Finally, it flows to the mixture chamber to be sampled. The clean air containing the odorant compound can be sampled through an indirect technique using a Tedlar bag and a Teflon tubing, to be posterior conducted to an analysis using, for example, gas chromatography. The shape of the mixture chamber was designed to avoid interferences of compounds coming from outside of the device (Jiang *et al.*, 1995). The dimensions of the PWT configuration to be used in the present work are shown in Figure 3. Its main section has 250 mm in height, 800 mm in length, and 400 mm in width.

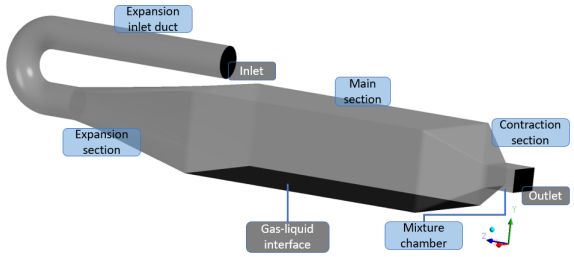

(a)

Figure 2: Isometric view of the PWT configuration used in the present work.

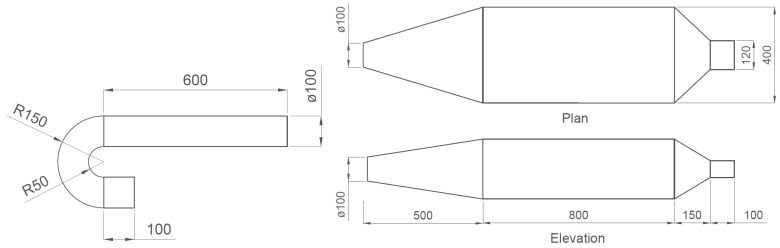

(a) (b)

Figure 3: Dimensions (in mm) of the PWT used used in the present work: (a) Extension inlet duct and (b) Device in it self.

2.2 Mathematical methodology

The airflow inside both geometries, PWT and U-Bend, is described through the Navier-Stokes equations since the fluid is Newtonian and incompressible. The flow inside both geometries is turbulent. To model the fluctuating effects it was used a RANS model, called the $SST\ \kappa-\omega$ (*SST - Shear Stress Transport*), proposed by Menter (1994). Specifically for the simulations concerning the U-bend flow, it was also tested the use of the $standard\ \kappa-\varepsilon$ model. After the appropriate statistical treatment, the equations for the transport of mass and momentum gets the form shown in Equations 1a and 1b, respectively. Whereas, for the $SST\ \kappa-\omega$ model, the values for κ, ω are obtained from their transport equations, shown in Equations 2a and 2b.

$$\frac{\partial \overline{u}}{\partial x_i} = 0 \tag{1a}$$

$$\rho\frac{\partial \overline{u}_i}{\partial t} + \rho\overline{u}_j\frac{\partial \overline{u}_i}{\partial x_j} = -\frac{\partial \overline{P}}{\partial x_i} + \frac{\partial}{\partial x_j}\left[\mu\left(\frac{\partial \overline{u}_i}{\partial x_j} + \frac{\partial \overline{u}_j}{\partial x_i}\right) - \rho\overline{u_i' u_j'}\right] \tag{1b}$$

where u_i is the velocity vector, ρ is the density of the fluid, μ is kinenamatic viscosity, μ_T is the turbulent viscosity, P is the pressure, t is the time and x_i is the position vector.

$$\frac{\partial \rho\kappa}{\partial t} + u_j\frac{\partial \rho\kappa}{\partial x_j} = \tau_{i,j}\frac{\partial u_i}{\partial x_j} - \beta^*\rho\omega\kappa + \frac{\partial}{\partial x_j}\left[(\mu + \sigma_\kappa\mu_T)\frac{\partial \kappa}{\partial x_j}\right] \tag{2a}$$

$$\frac{\partial \rho\omega}{\partial t} + u_j\frac{\partial \rho\omega}{\partial x_j} = \frac{\gamma}{\upsilon_t}\tau_{i,j}\frac{\partial u_i}{\partial x_j} - \beta\rho\omega^2 + \frac{\partial}{\partial x_j}\left[(\mu + \sigma_w\mu_T)\frac{\partial \omega}{\partial x_j}\right] + 2(1-F_1)\rho\sigma_\omega 2\frac{1}{\omega}\frac{\partial k}{\partial x_j}\frac{\partial \omega}{\partial x_j} \tag{2b}$$

where for conciseness, the reader is reffered to Menter (1994) for more details concerning the constants and functions of the model.

In the U-bend simulations, a fully developed velocity profile with an average value of $0.6\ m\ s^{-1}$ was set at the inlet. This velocity profile was experimentally obtained using the magnetic resonance velocimetry (MRV) technique, the data is presented by Benson *et al.* (2020). The no-slip condition was used on the walls. At the outlet, the atmospheric pressure condition was set. For the inlet profiles of the turbulence variables (κ, ω and ε) fully developed profiles were set at the

inlet. The average value of κ were equal to $0.027\ m^2\ s^{-2}$, ε were equal to $0.054\ m^2\ s^{-3}$ and for ω were equal to $237.55\ s^{-1}$.

Where in the PWT simulations, at the inlet a fully developed profile with an average value of $2.82\ m\ s^{-1}$ was set to achieve $0.3\ m\ s^{-1}$ as a mean velocity over the cross-section area in the main section of the tunnel. This value is presented by Jiang *et al.* (1995), i.e. the source of the experimental data to validate the results. The no-slip condition was used on the walls and at the outlet, and the atmospheric pressure condition. To the turbulence inlet parameters, i.e. the turbulent kinetic energy (κ) and its specific dissipation rate (ω), fully developed profiles of both variables were set at the inlet. The average value of κ were equal to $0.056\ m^2\ s^{-2}$ and of ω were equal to $1530.28\ s^{-1}$.

To solve the transport equations, the software *ANSYS Fluent* version 19.0 was used. This software is based on the finite volume method (Fluent, 2005), which is used mainly for the numerical solution of problems in fluid mechanics (Schäfer, 2006).

The gradients are solved using the least square cell-based method and the pressure terms using a second-order approach. The transient formulation was solved using a first-order implicit scheme, that method is recommended by the *ANSYS Fluent* User's Guide for most of the problems (Fluent *et al.*, 2011). It presents a lower computational cost when compared to the second-order version and presents reliable results. The pressure-velocity coupling is solved using the SIMPLE scheme. To interpolate the convective terms of the equations of momentum, turbulent kinetic energy, and its specific dissipation rate it was tested three different methodologies. The first and second order upwind and the use of a discretization blending factor of the first and second order upwind methods.

For each cell face, the First-to-Higher Order Blending obtains a blending of the flux from a low order scheme ($\varphi_{1st\ order}$) and a more accurate higher-order scheme ($\varphi_{2nd\ order}$). As shown in Equation 3, the use of a blending factor (B) of 0 reduces the gradient reconstruction to a low order discretization scheme and a value of 1 recovers the high order scheme (Papadakis and Bergeles, 1995). The *ANSYS Fluent* User's Guide recommends the use of a blending factor typically equal to 0.75 or 0.5 (Fluent *et al.*, 2011). For the present work, the use of a blending factor equal to 0.75 led to the convergence. The low-order scheme was first-order and the high-order scheme, a second-order.

$$\varphi = \varphi_{1st\ order} - B(\varphi_{2nd\ order} - \varphi_{1st\ order}) \tag{3}$$

To determine the time step size, it was used the adaptive time-stepping technique. In where there is no specification of a singular time step, but an interval (10^{-6} to 10^{-2}) and the time step is automatically determined based on the truncation error associated with the integration scheme. If the truncation error is smaller than a specified tolerance the time step is increased and on the other side, if the truncation error is higher than the tolerance the time step is decreased. It was used the truncation tolerance error equal to 0.01. The convergence criteria are the root mean square of the residual of each equation, which should be lower than 10^{-4}. This value is considered reasonable for many applications (Fluent, 2005). The time of simulation was calculated based on a characteristic length ($L^*\ [m]$) and a characteristic velocity ($u^*\ [m\ s^{-1}]$). Using these parameters, a characteristic time ($t^*\ [s]$) was calculated using the Equation 4. To guarantee the development of the airflow, it was calculated $200t^*$ as a stabilization time, and more $200t^*$ to collect data for time statistics.

$$t^* = \frac{L^*}{u^*} \tag{4}$$

where L^* is equal to the PWT main section height ($0.25\ m$) and u^* is an average velocity in the main section, equal to $0.2\ m\ s^{-1}$. Therefore, the characteristic time was equal to $1.25\ s$.

Both geometries were discretized using structured meshes, as shown in Figures 4. It was used $932,640$ cells for the PWT and $3,381,360$ for the U-bend when using the $SST\ \kappa - \omega$ model and $280,575$ when using the $standard\ \kappa - \varepsilon$ model.

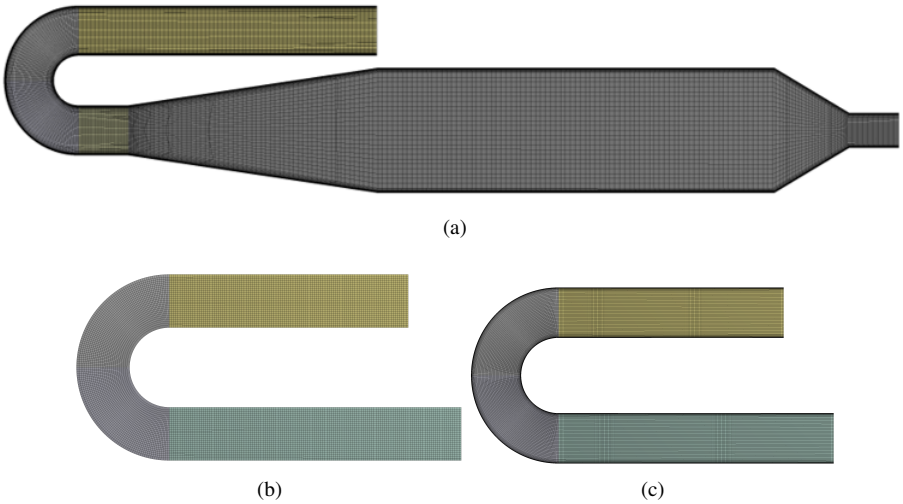

(a) (b) (c)

Figure 4: Lateral view of the discretized domains used in the present work: (a) PWT ($932,640 cells$); (b) U-bend $SST\ \kappa-\omega$ ($338,1360 cells$) and (c) U-bend $standard\ \kappa-\varepsilon$ ($280,575 cells$).

Grid independence tests were conducted for all the cases. For the simulations with the U-bend, six meshes with different resolutions were constructed to simulate the flow using the $SST\ \kappa-\omega$ model and three using the $\kappa-\varepsilon$ model. For the simulations using the $SST\ \kappa-\omega$ model, the coarsest mesh has $190,464$ elements, the coarser mesh has $465,320$ elements, the coarse mesh has $761,484$ elements, the medium mesh has $1,436,180$ elements, the fine mesh have $3,381,360$ elements and the finer mesh have $7,122,720$ elements. For the simulations using the $\kappa-\varepsilon$ model, the coarse mesh has $33,792$ elements, the medium mesh has $93,328$ and the fine mesh has $280,575$. The meshes' sensitivity was evaluated for the velocity and TKE. For the PWT simulations, to evaluate the sensitivity of the meshes, five meshes with different resolutions were constructed to simulate the airflow. The coarser mesh has $150,968$ elements, the coarse mesh has $282,576$ elements, the medium mesh has $434,112$ elements, the fine mesh has $932,640$ elements and the finer mesh has $1,808,940$ elements.

3. RESULTS

Benson *et al.* (2020) presents its experimental velocity profiles in the four cross-sections, shown in Figure 5-a and 5-b, being $H = 25\ mm$. Each cross-section was divided into three lines (Figure 5-b), the u component of the velocity was present at the $z'/H = 0$, the v component at the $y'/H = -0.4$ and w component at the $y'/H = -0.3$. The numerical results to be compared with the experimental data were taken following the same methodology.

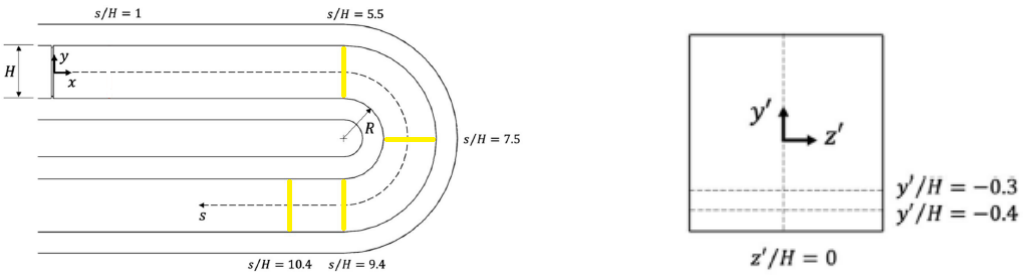

(a) (b)

Figure 5: Sampling lines cross-section: (a) Lateral view and (b) Frontal view.

Figure 6 shows, for both turbulence models, the velocity profiles for the u component. Analyzing the $\kappa-\varepsilon$ results in the region before the U-bend curve ($z = 55\ mm$) and far from the walls, y'/H approximately between -0.35 and 0.35, this model showed a good correspondence with the $SST\ \kappa-\omega$ and the experimental results. However, the results in the middle of the U-bend curve ($z = 75\ mm$) and after it ($z = 94$ and $104\ mm$, respectively), do not show the same good correspondence. There was a lack of accuracy far and close to the walls. On the other hand, by analyzing the $SST\ \kappa-\omega$ results, it can be seen that, in general, this model can capture all the tendencies of the flow with considerable accuracy. Furthermore, the $\kappa-\varepsilon$ results show a considerable difference between numerical and experimental data in the near-wall region. In this region, close to the walls, there is a considerable difference between the accuracy of the two models' results, which can be explained by the fundamental differences in the models to account for the near-wall region flow characteristics. The $SST\ \kappa-\omega$ model directly applies the no-slip condition and therefore directly calculates the

near-wall flow, while the $\kappa - \varepsilon$ model uses wall functions to describe the flow in this region. As explained by Eça *et al.* (2015), the advantage of the use of these models is purely numerical. In addition, the use of the $\kappa - \varepsilon$ model is not adequate to simulate the flow in adverse pressure gradients and close to walls (Santos *et al.*, 2009; Wilcox *et al.*, 1998; Menter, 1994), such as the characteristic of the flow and geometry of the U-bend. Therefore, given the results obtained for the U-bend simulations and the literature review, the $SST\ \kappa - \omega$ model was chosen to perform the PWT simulations. For an analysis of the numerical results for the other components of the velocity, the reader is referred to Siqueira (2022).

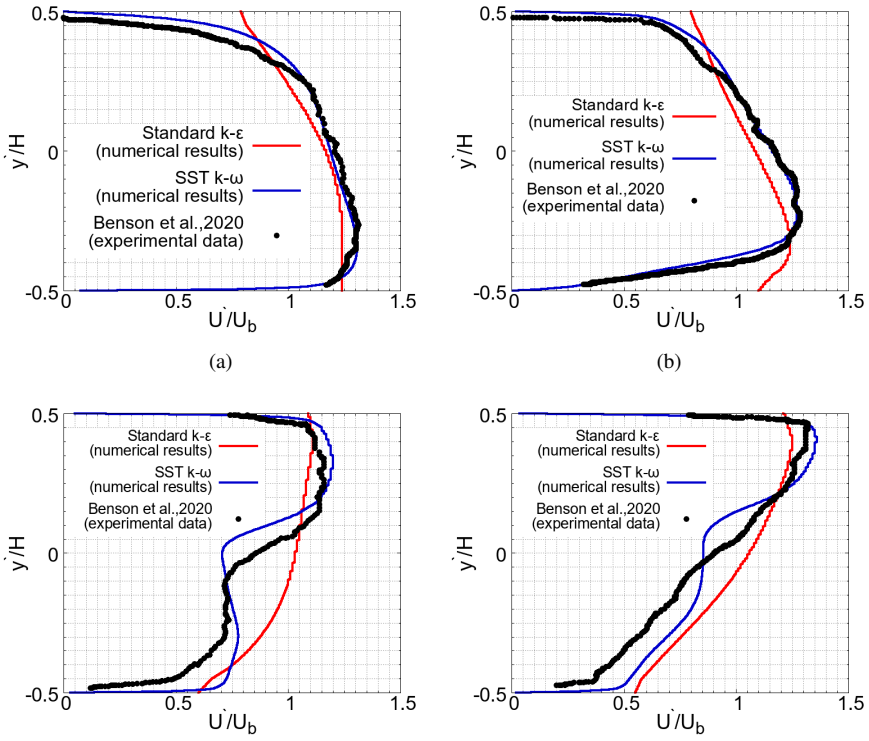

Figure 6: Benson *et al.* (2020) U bend validation for both turbulence models - u component of the velocity profiles at the positions: (a)$z = 55\ mm$; (b)$z = 75\ mm$; (c) $z = 94\ mm$ and (d) $z = 104\ mm$.

The flow inside the PWT is validated using the Jiang *et al.* (1995) data. The velocity measurements were taken at three different cross-sections ($z = 200$, 400 and $600\ mm$) shown in Figure 7, in where the reference ($z = 0$) it is located at the starting point of the main section. Each cross-section was divided into 40 equally distant points, distant $50\ mm$ from each other. The horizontal velocity profile was calculated by averaging the velocities at 5 different heights for each horizontal level at each position.

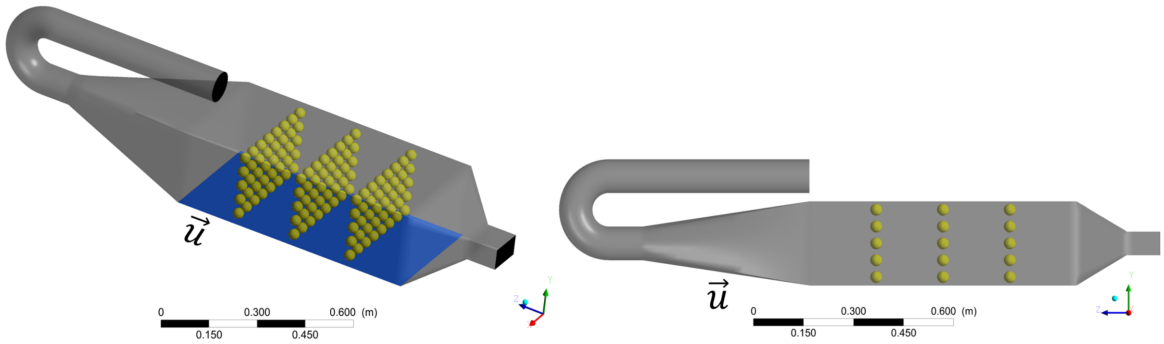

Figure 7: Sampling points in the three cross-sections: (a)Isometric view and (b) lateral view.

Figure 8 shows the comparison between the vertical profiles obtained by the numerical simulations for $\overline{u}$ and the experimental data, while Figure 9 shows the correlation coefficients. It can be seen that, despite the problems related to the Jiang *et al.* (1995) experiments and data, already discussed in Section 1, a good correspondence between the numerical

and experimental data was achieved. Ratner (2009) points out that correlation coefficient (R^2) values between 0.7 and 1.0 indicates a strong relation.

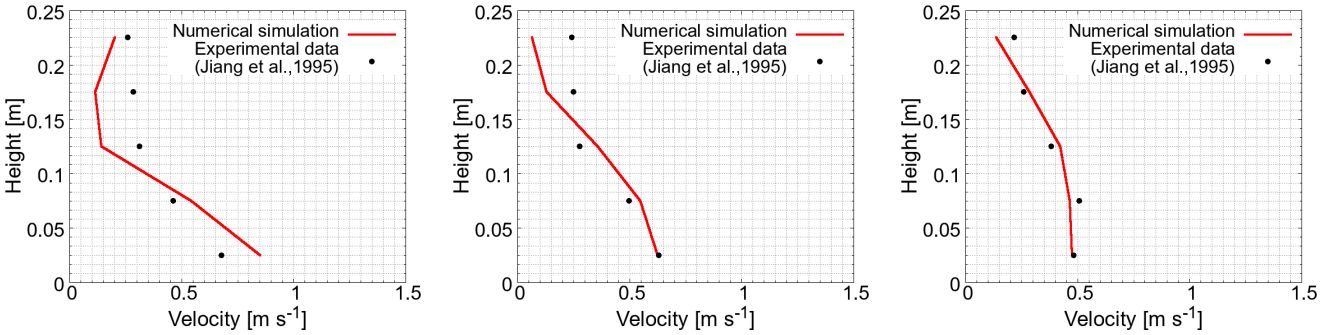

(a) (b) (c)

Figure 8: Vertical profiles for $\overline{u}$ - numerical results compared to the experimental data at the positions: (a) $z = 200\ mm$; (b) $z = 400\ mm$ and (c) $z = 600\ mm$.

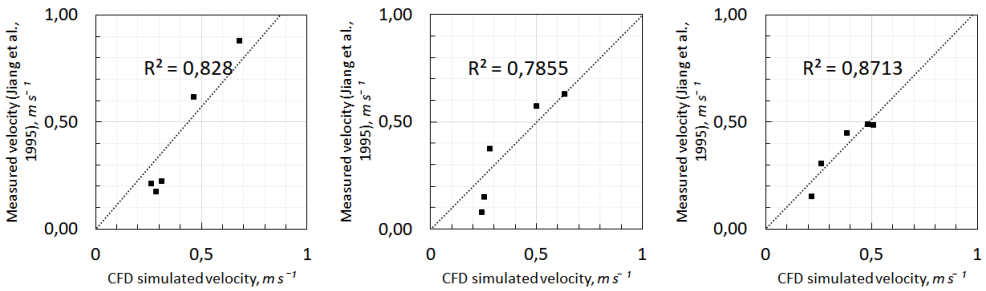

(a) (b) (c)

Figure 9: Vertical profiles for $\overline{u}$ - Correlation coefficient for the numerical results compared to the experimental data: (a) $z = 200\ mm$; (b) $z = 400\ mm$ and (c) $z = 600\ mm$.

Figures 11 and 12 present the velocity profiles and distribution, respectively, when using a pure first and second-order upwind discretization and a discretization blending factor between the two equal to 0.75. At first sight, looking only at the velocity profiles, it can be seen that the best results are obtained when using second-order upwind discretization. However, looking at the velocity distribution a convergence problem is perceived. The results when using a pure second-order upwind discretization aren't symmetric, which is expected for this kind of airflow and geometry. The velocity profiles aren't capable to show this issue probably because of the way they are obtained, i.e. averaging the velocity values along a cross-section. This convergence problem, when using the second-order upwind method, seems to happen due to the airflow complexity, (i.e. $3D$ and with several re-circulation zones, for instance - shown in Figure 10), which is caused by the PWT geometry, especially by the presence of curves, walls, expansions, and contraction.

On the other hand, the results when using first-order schemes although producing a good convergence weren't showing great accuracy when compared to the experimental results, presented by Jiang *et al.* (1995). In summary, although the results obtained when using the second-order schemes presents great accuracy, it also leads to convergence problems. For the first-order schemes was the opposite, with great convergence and a lack of accuracy. In such cases, the *ANSYS Fluent* User's Guide recommends the use of a discretization blending factor (Fluent *et al.*, 2011). Looking for both results, velocity profiles, and distribution, the use of a blending factor equal to 0.75 led to the convergence maintaining a great accuracy when compared to first-order upwind results.

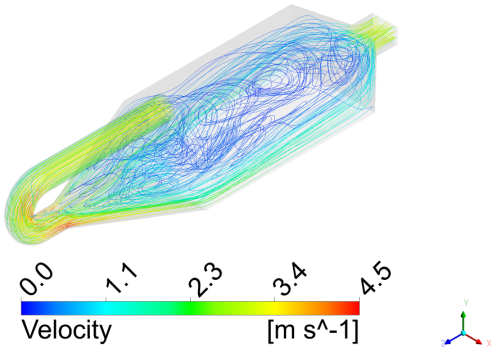

Figure 10: Streamlines isometric view - Jiang *et al.* (1995) PWT simulations.

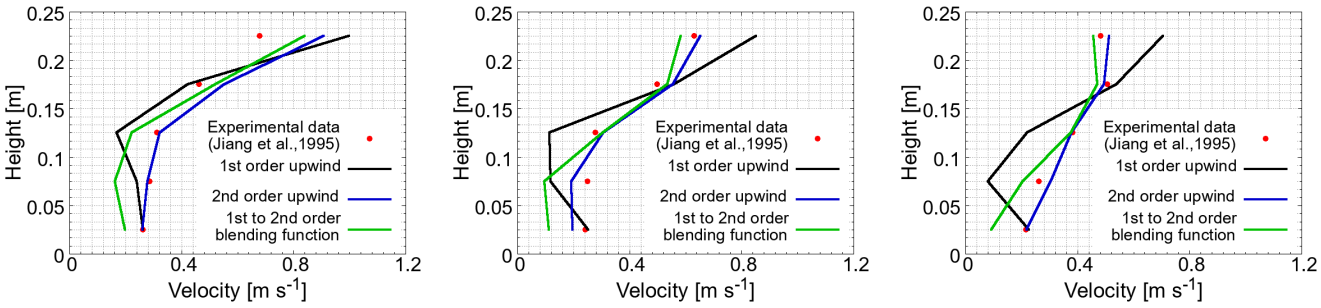

(a) (b) (c)

Figure 11: Vertical profiles for $\overline{u}$ for the three discretization methods analyzed - numerical results compared to the experimental data at the positions: (a) $z = 200\ mm$; (b) $z = 400\ mm$ and (c) $z = 600\ mm$.

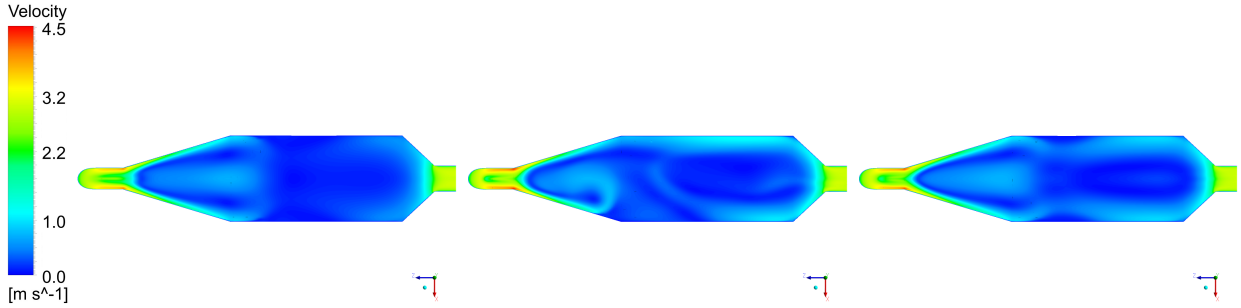

(a) (b) (c)

Figure 12: Velocity distribution for $\overline{u}$ top view at half of the PWT height ($y = 125$) - Jiang *et al.* (1995) PWT simulations for different methods: (a) First order upwind; (b) Second order upwind and (c) Blending function between the two equal to 0.75.

4. CONCLUSIONS

The objectives of this work were to test two different turbulence models, $standard\ \kappa - \epsilon$ and the $SST\ \kappa - \omega$, to simulate the flow inside a U-bend when compared to the experimental presented by Benson *et al.* (2020). And also to test three different discretization methods for the convective terms of the equations of momentum, turbulent kinetic energy, and its dissipation rate to simulate the airflow inside the PWT. It was tested the first-order upwind, a second-order upwind, and the use of a discretization blending factor between the two equal to 0.75. About the U-bend simulations, the best results were found when using the $SST\ \kappa - \omega$ model and using a structured mesh. For the PWT simulations, a better convergence and maintaining a relatively great accuracy, when compared to the Jiang *et al.* (1995) data, were obtained when using the discretization blending factor equal to 0.75.

The author(s) is (are) solely responsible for the printed material included in this paper.

5. ACKNOWLEDGEMENTS

The authors would like to acknowledge the CNPq (Conselho Nacional de Desenvolvimento Científico e Tecnológico), so as to the Fapes (Fundação de Amparo à Pesquisa e Inovação do Espírito Santo) and the CAPES (Coordenação de Aperfeiçoamento de Pessoal de Nível Superior).

6. REFERENCES

Beghi, S.P., Santos, J.M., Reis, N.C., de Sá, L.M., Goulart, E.V. and de Abreu Costa, E., 2012. "Impact assessment of odours emitted by a wastewater treatment plant". *Water Science and Technology*, Vol. 66, No. 10, pp. 2223–2228.

Benson, M.J., Banko, A.J., Elkins, C.J., An, D.G., Song, S., Bruschewski, M., Grundmann, S., Borup, D.D. and Eaton, J.K., 2020. "The 2019 mrv challenge: turbulent flow through a u-bend". *Experiments in Fluids*, Vol. 61, pp. 1–17.

Capelli, L., Sironi, S., Del Rosso, R. and Céntola, P., 2009. "Predicting odour emissions from wastewater treatment plants by means of odour emission factors". *Water research*, Vol. 43, No. 7, pp. 1977–1985.

Daelman, M.R., van Voorthuizen, E.M., van Dongen, U.G., Volcke, E.I. and van Loosdrecht, M.C., 2012. "Methane emission during municipal wastewater treatment". *Water research*, Vol. 46, No. 11, pp. 3657–3670.

Eça, L., Saraiva, G., Vaz, G. and Abreu, H., 2015. "The pros and cons of wall functions". In *International Conference on Offshore Mechanics and Arctic Engineering*. American Society of Mechanical Engineers, Vol. 56482, p. V002T08A012.

Fluent, 2005. "Manual and user guide of fluent software". *Fluent Inc*, Vol. 597.

Fluent, A. *et al.*, 2011. "Ansys fluent theory guide". *ANSYS Inc., USA*, Vol. 15317, pp. 724–746.

Glaz, P., Bartosiewicz, M., Laurion, I., Reichwaldt, E.S., Maranger, R. and Ghadouani, A., 2016. "Greenhouse gas emissions from waste stabilisation ponds in western australia and quebec (canada)". *Water research*, Vol. 101, pp. 64–74.

Godoi, A.F.L., Grasel, A.M., Polezer, G., Brown, A., Potgieter-Vermaak, S., Scremim, D.C., Yamamoto, C.I. and Godoi, R.H.M., 2018. "Human exposure to hydrogen sulphide concentrations near wastewater treatment plants". *Science of the Total Environment*, Vol. 610, pp. 583–590.

Gostelow, P., Parsons, S. and Stuetz, R., 2001. "Odour measurements for sewage treatment works". *Water research*, Vol. 35, No. 3, pp. 579–597.

Hayes, J., Stevenson, R. and Stuetz, R., 2014. "The impact of malodour on communities: A review of assessment techniques". *Science of the Total Environment*, Vol. 500, pp. 395–407.

Hu, L., Du, Y. and Long, Y., 2017. "Relationship between h2s emissions and the migration of sulfur-containing compounds in landfill sites". *Ecological Engineering*, Vol. 106, pp. 17–23.

Jiang, K., Bliss, P.J. and Schulz, T.J., 1995. "The development of a sampling system for determining odor emission rates from areal surfaces: Part i. aerodynamic performance". *Journal of the Air & Waste Management Association*, Vol. 45, No. 11, pp. 917–922.

Jiang, K. and Kaye, R., 1996. "Comparison study on portable wind tunnel system and isolation chamber for determination of vocs from areal sources". *Water Science and Technology*, Vol. 34, No. 3-4, p. 583.

Lebrero, R., Bouchy, L., Stuetz, R. and Muñoz, R., 2011. "Odor assessment and management in wastewater treatment plants: a review". *Critical Reviews in Environmental Science and Technology*, Vol. 41, No. 10, pp. 915–950.

Martins, R., Siqueira, M., Toniato, I., Cupertino, K., Junior, A.P., Neyval, J.R., Stuetz, R. and Santos, J., 2018. "Evaluating the flow inside of portable wind tunnels for odour measurements". *Chemical Engineering Transactions*, Vol. 68, pp. 55–60.

Menter, F.R., 1994. "Two-equation eddy-viscosity turbulence models for engineering applications". *AIAA journal*, Vol. 32, No. 8, pp. 1598–1605.

Papadakis, G. and Bergeles, G., 1995. "A locally modified second order upwind scheme for convection terms discretization". *International Journal of Numerical Methods for Heat & Fluid Flow*.

Prata Jr, A.A., Lucernoni, F., Santos, J.M., Capelli, L., Sironi, S., Le-Minh, N. and Stuetz, R.M., 2018. "Mass transfer inside a flux hood for the sampling of gaseous emissions from liquid surfaces–experimental assessment and emission rate rescaling". *Atmospheric environment*, Vol. 179, pp. 227–238.

Ratner, B., 2009. "The correlation coefficient: Its values range between+ 1/- 1, or do they?" *Journal of targeting, measurement and analysis for marketing*, Vol. 17, No. 2, pp. 139–142.

Santos, J.M., Reis Jr, N.C., Goulart, E.V. and Mavroidis, I., 2009. "Numerical simulation of flow and dispersion around an isolated cubical building: The effect of the atmospheric stratification". *Atmospheric Environment*, Vol. 43, No. 34, pp. 5484–5492.

Schäfer, M., 2006. *Computational engineering: Introduction to numerical methods*, Vol. 321. Springer.

Schiffman, S.S. and Williams, C.M., 2005. "Science of odor as a potential health issue". *Journal of environmental quality*, Vol. 34, No. 1, pp. 129–138.

Siqueira, M.d.A., 2022. *INFLUENCE OF THE DESIGN AND OPERATIONAL CONDITIONS ON THE AIRFLOW*

AND MASS TRANSFER PHENOMENA INSIDE A PORTABLE WIND TUNNEL USED TO ESTIMATE ODORANT COMPOUNDS MEASURED OVER PASSIVE LIQUID SURFACES. Master's thesis, Universidade Federal do Espírito Santo.

Wilcox, D.C. *et al.*, 1998. *Turbulence modeling for CFD*, Vol. 2. DCW industries La Canada, CA.

Yang, W.B., Chen, W.H., Yuan, C.S., Yang, J.C. and Zhao, Q.L., 2012. "Comparative assessments of voc emission rates and associated health risks from wastewater treatment processes". *Journal of Environmental Monitoring*, Vol. 14, No. 9, pp. 2464–2474.

7. RESPONSIBILITY NOTICE

The authors are solely responsible for the printed material included in this paper.